Helical temperature perturbations associated with radially asymmetric magnetic island chains in tokamak plasmas

Richard Fitzpatrick

Citation: Physics of Plasmas **23**, 122502 (2016); doi: 10.1063/1.4968833
View online: http://dx.doi.org/10.1063/1.4968833
View Table of Contents: http://scitation.aip.org/content/aip/journal/pop/23/12?ver=pdfcov
Published by the AIP Publishing

Helical temperature perturbations associated with radially asymmetric magnetic island chains in tokamak plasmas

Richard Fitzpatrick
Department of Physics, Institute for Fusion Studies, University of Texas at Austin, Austin, Texas 78712, USA

(Received 19 August 2016; accepted 8 November 2016; published online 5 December 2016)

The simple analysis of Rutherford [Phys. Fluids **16**, 1903 (1973)] is generalized in order to incorporate radial magnetic island asymmetry into the nonlinear theory of tearing mode stability in a low-β, large aspect-ratio, quasi-cylindrical, tokamak plasma. The calculation is restricted to cases in which the radial shifts of the island X- and O-points are (almost) equal and opposite. For the sake of simplicity, the calculation concentrates on a particular (but fairly general) class of radially asymmetric island magnetic flux-surfaces that can all be mapped to the same symmetric flux-surfaces by means of a suitable coordinate transform. The combination of island asymmetry (in which the radial shifts of the X- and O-points are almost equal and opposite) and temperature-induced changes in the inductive current profile in the immediate vicinity of the island is found to have no effect on tearing mode stability. *Published by AIP Publishing.* [http://dx.doi.org/10.1063/1.4968833]

I. INTRODUCTION

A tokamak is a device that is designed to trap a thermonuclear plasma on a set of toroidally nested magnetic flux-surfaces.[1] Heat is able to flow around the flux-surfaces relatively rapidly due to the free streaming of charged particles along magnetic field-lines. On the other hand, heat is only able to diffuse across the flux-surfaces relatively slowly, assuming that the magnetic field-strength is large enough to render the particle gyroradii much smaller than the device's minor radius.[2] Another way of saying this is that if the particle gyroradii are relatively small then the thermal conductivity of the plasma parallel to magnetic field-lines, $\kappa_\parallel$, exceeds that perpendicular to magnetic field-lines, $\kappa_\perp$, by many orders of magnitude.[3] (This remains true even when the enhancement of perpendicular heat transport due to small-scale plasma turbulence is taken into account.[4]) Hence, the plasma temperature gradients within magnetic flux-surfaces are usually very much smaller than those across the surfaces: i.e., the temperature is a flux-surface function.

Tokamak plasmas are subject to a number of macroscopic instabilities that limit their effectiveness.[5] So-called *tearing modes* are comparatively slowly growing instabilities[6,7] that tend to saturate at relatively low amplitudes,[8–10] in the process reconnecting magnetic flux-surfaces to form helical structures known as *magnetic island chains*. Magnetic island chains are radially localized structures centered on so-called *rational magnetic flux-surfaces*, which satisfy $\mathbf{k}\cdot\mathbf{B}=0$, where $\mathbf{k}$ is the wave-number of the instability and $\mathbf{B}$ the equilibrium magnetic field.

It turns out that the connection length (i.e., the typical distance that a charged particle must stream along a magnetic field-line in order to sample the whole flux-surface) is infinite on a rational magnetic flux-surface. This property allows perpendicular heat transport to be competitive with parallel heat transport in the immediate vicinity of such a surface, even in the limit that $\kappa_\parallel/\kappa_\perp \gg 1$. Indeed, it can be shown that perpendicular transport is significant inside a thin layer of characteristic radial thickness $W_c \propto (\kappa_\perp/\kappa_\parallel)^{1/4}$, centered on the rational surface, but is insignificant outside the layer.[4] It follows that the temperature is not necessarily a flux-surface function within the layer (although it has to be a flux-surface function outside the layer).

Consider an island chain whose magnetic separatrix encloses a region of the plasma, centered on the associated rational surface, and whose full radial width is W. In the so-called *wide-island limit*, $W \gg W_c$, the temperature profile inside the separatrix is constrained to be a flux-surface function. It follows that the temperature profile is largely flattened inside the separatrix, which implies a significant loss of energy confinement in the island region.[11] The flattening of the temperature profile also suppresses the non-inductive *bootstrap current*[12] within the magnetic separatrix—an effect that is known to have a strong destabilizing effect on the associated tearing perturbation.[13] On the other hand, in the so-called *narrow-island limit*, $W \ll W_c$, the temperature profile inside the separatrix is not constrained to be a flux-surface function. It follows that the temperature profile is not flattened within the separatrix (in fact, it is almost completely unaffected by the island chain), so there is no loss of energy confinement, and no destabilizing effect due to a localized suppression of the bootstrap current.[4]

The conventional analysis of the localized (about the rational surface) temperature perturbations induced in a tokamak plasma by a magnetic island chain[4] assumes that the chain is *radially symmetric*: in other words, that the region of the plasma enclosed by the magnetic separatrix is bisected by the (unperturbed) rational surface. However, there is clear experimental evidence that this is not generally the case. Indeed, electron cyclotron emission (ECE) data reveal that, for the case of a low wave-number magnetic island chain, the region of the plasma enclosed by the magnetic separatrix that is situated inside the (unperturbed) rational surface is typically greater in radial extent than the corresponding region situated outside the surface.[14] This asymmetry is associated with an inward radial shift (relative to the rational

surface) of the island O-points and an outward shift of the X-points. Theoretically, radial island asymmetry can be accounted for in terms of a finite mean gradient of the linearized tearing mode eigenfunction at the rational surface.[15,16]

In principle, the radial asymmetry of a typical magnetic island chain in a tokamak plasma can modify the stability of the associated tearing instability. Such a modification can occur via one of the two mechanisms, both of which are associated with the modified temperature perturbation associated with island asymmetry. The first mechanism is via changes in the non-inductive bootstrap current density profile in the immediate vicinity of the island chain (this profile depends on the plasma pressure gradient, which, in turn, depends on the plasma temperature) and the second is via changes in the inductive current density profile (this profile depends on the plasma electrical conductivity, which, in turn, depends on the plasma temperature). The first mechanism is expected to be relatively unimportant, because the perturbed bootstrap current density profile associated with a radially symmetric island chain already has a significant destabilizing influence on the associated tearing instability, and, to lowest order, the modification to this influence due to island asymmetry should vanish by symmetry. On the other hand, the second mechanism could possibly be important, because, by symmetry, the perturbed inductive current density profile associated with a radially symmetric island chain has zero influence on the stability of the associated tearing instability, whereas the modification to this influence due to island asymmetry does not obviously vanish by symmetry.

Reference 10 reports that, in the narrow-island limit, the aforementioned second mechanism gives rise to a significant destabilizing term in the so-called *Rutherford island width evolution equation*[7] (which governs nonlinear tearing mode stability) that is proportional to the degree of radial asymmetry. Furthermore, Ref. 17 reports that, in the wide-island limit, the second mechanism also gives rise to a significant destabilizing term in the Rutherford equation that is proportional to the radial asymmetry. However, somewhat confusingly, Ref. 10 claims that the term in question is nonexistent in the wide-island limit. The destabilizing term found in Ref. 17 is of particular importance because it plays a crucial role in a recently developed theory of density limit disruptions in tokamak plasmas.[17–21]

The aim of this paper is to incorporate radial island asymmetry into the simple theory of nonlinear tearing mode stability in tokamak plasmas due to Rutherford,[7] in a (not entirely successful) attempt to resolve the aforementioned disagreement between the results of Refs. 10 and 17.

This paper is organized as follows. Section II outlines the conventional, large aspect-ratio, quasi-cylindrical, low-β, constant-ψ, resistive-magnetohydrodynamic (MHD) model that is used to analyze tearing mode stability. Section III derives a closed set of equations, from the aforementioned model, that allow the various terms in the Rutherford equation of a particular class of radially asymmetric magnetic island chains to be calculated. These equations are solved in the narrow-island limit in Sec. IV and in the wide-island limit in Sec. V. The paper is summarized, and conclusions are drawn, in Sec. VI.

II. PRELIMINARY ANALYSIS

A. Fundamental definitions

Consider a large aspect-ratio, low-β, circular cross-section, tokamak plasma equilibrium. Let us adopt a right-handed cylindrical coordinate system (r, θ, z) whose symmetry axis $(r=0)$ coincides with the magnetic axis of the plasma. The system is assumed to be periodic in the z-direction with period $2\pi R_0$, where R_0 is the simulated major plasma radius. It is helpful to define the simulated toroidal angle $\varphi = z/R_0$. The coordinate r serves as a label for the unperturbed (by the tearing mode) magnetic flux-surfaces. Let the equilibrium toroidal magnetic field, B_z, and the equilibrium toroidal plasma current both run in the $+z$ direction.

Suppose that a tearing mode generates a helical magnetic island chain, with m_θ poloidal periods, and n_φ toroidal periods, that is embedded in the aforementioned plasma. The island chain is assumed to be radially localized in the vicinity of its associated rational surface, minor radius r_s, which is defined as the unperturbed magnetic flux-surface at which $q(r_s) = m_\theta/n_\varphi$. Here, $q(r)$ is the safety-factor profile (which is assumed to be a monotonically increasing function of r). Let the full radial width of the island chain's magnetic separatrix be $4w$. In the following, it is assumed that $\epsilon_s \equiv r_s/R_0 \ll 1$ and $w/r_s \ll 1$.

B. Asymptotic matching

The system is conveniently divided into an inner region that comprises the plasma in the immediate vicinity of the rational surface (and includes the island chain) and an outer region that comprises the remainder of the plasma. As is well known, in a high-temperature tokamak plasma, linear ideal-MHD analysis invariably suffices to calculate the mode structure in the outer region, whereas nonlinear resistive-MHD analysis is generally required in the inner region. The complete solution is obtained by asymptotically matching the linear solution in the outer region to the nonlinear solution in the inner region.

The simplest asymptotic matching scheme is the so-called "lowest-order" scheme in which the finite width of the island is neglected when calculating the linear solution in the outer region. The linear solution is characterized by a real parameter, Δ', (with units of inverse length) known as the tearing stability index.[6] (see Sec. II E.) Lowest-order asymptotic matching is suitable for making a relatively quick determination as to whether or not a given physical mechanism would cause the width of a narrow island to spontaneously increase or decrease. For example, lowest-order asymptotic matching has been successfully used to demonstrate that the linear Δ' gives rise to a constant term in the Rutherford island width evolution equation,[7] that the loss of the bootstrap current inside a magnetic island associated with temperature flattening gives rise to a destabilizing term that scales as $1/w$,[13] and that magnetic curvature gives rise to a stabilizing term that scales as $1/w$.[22] Unfortunately, a lowest-order asymptotic matching scheme is incapable of accounting for the terms in the Rutherford island width evolution equation that usually give rise to the eventual

saturation of the island. These terms tend to vary as $w \ln w$, or w, or w^2, and can only be found via "higher-order" matching schemes in which the finite width of the island is taken into account when calculating the linear solution in the outer region.[8–10] Higher-order matching schemes are much more difficult to implement that the lowest-order scheme because they invariably involve iteration (since the finite island width solution in the outer region depends on the solution in the inner region, and vice versa). It follows, from the previous discussion, that the Rutherford island width evolution equation obtained from lowest-order asymptotic matching is generally only valid when the island width is significantly less than its final saturated value (because the saturation terms can be neglected in this limit).

In this paper, we are primarily interested in determining whether or not radial island asymmetry gives rise to a strongly destabilizing term in the Rutherford island width evolution equation, rather than calculating the final saturated width of the island. Lowest-order asymptotic matching is perfectly capable of making such a determination and is, therefore, the matching scheme adopted in the following analysis.

C. Resistive-MHD equations

It is convenient to employ a frame of reference in the inner region that co-rotates with the magnetic island chain. All fields in the inner region are assumed to depend (spatially) only on the radial coordinate $x = r - r_s$ and the helical angle $\zeta = m_\theta\,\theta - n_\varphi\,\varphi$. The governing equations in the inner region take the form[23]

$$\partial_t \chi = \{\Phi, \chi\} - \eta(T)\,\delta j_{bz} - \eta(T)\,j_z + \eta(T_s)\,j_{z0}, \tag{1}$$

$$\rho\,\partial_t\,\omega_z = \rho\,\{\Phi, \omega_z\} + \{j_z, \chi\}, \tag{2}$$

$$\partial_t E = \{\Phi, E\} + \frac{\kappa_\parallel}{B_z^2}\{\{T, \chi\}, \chi\} + \kappa_\perp\,\partial_x^2 T + \eta(T) j_z^2 - \eta(T_s) j_{z0}^2, \tag{3}$$

$$\mu_0 j_z = -\nabla^2 \chi + \frac{2\,B_z}{R_0\,q_s}, \tag{4}$$

$$\mu_0 j_{z0} = \frac{B_z}{R_0\,q_s}\,(2 - s_s), \tag{5}$$

$$\omega_z = -\nabla^2 \Phi. \tag{6}$$

Here,

$$\{A, B\} \equiv k_\theta(\partial_x A\,\partial_\zeta B - \partial_\zeta A\,\partial_x B), \tag{7}$$

where $k_\theta = m_\theta/r_s$, $q_s = m_\theta/n_\varphi$, $s_s = d\ln q/d\ln r|_{r_s}$, $\partial_t \equiv \partial/\partial t|_{x,\zeta}$, $\partial_x \equiv \partial/\partial x|_\zeta$, and $\partial_\zeta \equiv \partial/\partial\zeta|_x$. (All spatial derivates are taken at constant time.) Equation (1) is the toroidal component of Ohm's law, Eq. (2) the toroidal component of the vorticity equation, and Eq. (3) the energy conservation equation. Furthermore,

$$\chi = -\frac{B_z}{R_0}\int_0^x \left(\frac{1}{q} - \frac{1}{q_s}\right)(r_s + x)\,dx + \delta\mathbf{B}, \tag{8}$$

(where $\delta\mathbf{B}$ is the perturbed magnetic field) is the helical magnetic flux, Φ minus the scalar electric potential divided by B_z, η the resistivity, T the temperature, T_s the unperturbed temperature at the rational surface, j_z the toroidal current density, j_{z0} the unperturbed (by the tearing perturbation) toroidal current density, δj_{bz} the perturbed non-inductive bootstrap current density, ρ the mass density, ω_z the toroidal component of the vorticity, E the internal energy density, $\kappa_\parallel$ the parallel thermal conductivity, and $\kappa_\perp$ the perpendicular thermal conductivity. It is easily demonstrated that $\mathbf{B}\cdot\nabla\chi = 0$, which implies that χ is a magnetic flux-surface label. Note that, for the sake of simplicity, ρ, $\kappa_\parallel$, and $\kappa_\perp$ are all assumed to be spatially uniform constants. Moreover, we have taken ohmic heating into account, but have subtracted off the background (because the lowest-order asymptotic matching scheme cannot deal with a heat source in the inner region whose volume integral does not converge). The conventional (single-fluid) expression for the perturbed bootstrap current density is[24]

$$\delta j_{bz} = -f_s\,\frac{q_s}{\epsilon_s}\,\frac{n_s}{B_z}\left(\partial_x T + \frac{T_s}{L_T}\right), \tag{9}$$

where $f_s = 1.46\,\epsilon_s^{1/2}$ is the fraction of trapped particles, and n_s the electron number density (which is assumed to be spatially uniform and constant in the inner region). Finally, $L_T = -1/(d\ln T_0/dr)_{r_s}$ is the unperturbed (by the tearing mode) temperature gradient scale-length at the rational surface, where $T_0(r)$ is the unperturbed temperature profile. [Thus, $T_s = T_0(r_s)$.]

D. Normalization scheme

Let

$$X = \frac{x}{w}, \tag{10}$$

$$[A, B] \equiv \partial_X A\;\partial_\zeta B - \partial_\zeta A\;\partial_X B, \tag{11}$$

$$L_s = \frac{R_0\,q_s}{s_s}, \tag{12}$$

$$\psi = \frac{L_s}{B_z\,w^2}\,\chi, \tag{13}$$

$$J = \frac{\mu_0\,L_s}{B_z}\,j_z, \tag{14}$$

$$J_b = \frac{\mu_0\,L_s}{B_z}\,\delta j_{bz}, \tag{15}$$

$$\phi = \frac{\mu_0\,k_\theta\,w}{\eta(T_s)}\,\Phi, \tag{16}$$

$$U = \frac{\mu_0\,k_\theta\,w^3}{\eta(T_s)}\,\omega_z, \tag{17}$$

$$\mathcal{E} = \frac{\eta(T_s)}{\mu_0\,\kappa_\perp\,T_s}\,E, \tag{18}$$

$$\hat{T} = \frac{T}{T_s}, \tag{19}$$

$$\hat{\eta} = \frac{\eta(T)}{\eta(T_s)}. \tag{20}$$

Note that $\partial_X \equiv \partial/\partial X|_\zeta$ and $\partial_\zeta \equiv \partial/\partial\zeta|_X$. Moreover, L_s is the equilibrium magnetic shear-length at the rational surface. Equations (1)–(6) reduce to

$$\tau_R \frac{\partial}{\partial t}\left[\left(\frac{w}{r_s}\right)^2 \psi\right] = [\phi,\psi] - \hat{\eta}(\hat{T})\,(J - J_b) + \frac{2}{s_s} - 1, \quad (21)$$

$$\left(\frac{w}{r_s}\right)^5 \tau_R \frac{\partial}{\partial t}\left[\left(\frac{r_s}{w}\right)^3 U\right] = [\phi, U] + S^2 \left(\frac{w}{r_s}\right)^6 [J,\psi], \quad (22)$$

$$\left(\frac{w}{r_s}\right)^2 \tau_R \frac{\partial \mathcal{E}}{\partial t} = [\phi,\mathcal{E}] + \left(\frac{w}{w_c}\right)^4 [[\hat{T},\psi],\psi] + \partial_X^2 \hat{T} + \frac{\tau_E}{\beta\,\tau_R}\left(\frac{w}{L_s}\right)^2 \left[\hat{\eta}(\hat{T})\,J^2 - \left(\frac{2}{s_s} - 1\right)^2\right], \quad (23)$$

$$J \simeq -\partial_X^2 \psi + \frac{2}{s_s}, \quad (24)$$

$$J_b = -\alpha_b \left(\frac{L_s}{L_T} + \frac{L_s}{w}\,\partial_X \hat{T}\right), \quad (25)$$

$$U \simeq -\partial_X^2\,\phi. \quad (26)$$

Here,

$$S = \frac{\tau_R}{\tau_H}, \quad (27)$$

$$\tau_R = \frac{\mu_0\, r_s^2}{\eta(T_s)}, \quad (28)$$

$$\tau_H = \frac{L_s}{k_\theta\, r_s}\frac{\sqrt{\mu_0\,\rho}}{B_z}, \quad (29)$$

$$\tau_E = \frac{n_s\, r_s^2}{\kappa_\perp}, \quad (30)$$

are the Lundquist number, resistive diffusion time-scale, hydromagnetic time-scale, and energy confinement time-scale, respectively, at the rational surface. Moreover,

$$\alpha_b = f_s\,\frac{q_s}{\epsilon_s}\,\beta, \quad (31)$$

$$\beta = \frac{\mu_0\, n_s\, T_s}{B_z^2}. \quad (32)$$

Finally,[4]

$$w_c = \left(\frac{\kappa_\perp}{\kappa_\parallel}\right)^{1/4}\left(\frac{L_s}{k_\theta}\right)^{1/2}, \quad (33)$$

where $W_c = 4\,w_c$ is the critical island width mentioned in the Introduction.

E. Lowest-order asymptotic matching

Lowest-order asymptotic matching between the solutions in the inner and outer regions gives[6]

$$\Delta' w \simeq -2\int_{-\infty}^{\infty} J\cos\zeta\, dX\,\frac{d\zeta}{2\pi}. \quad (34)$$

F. Large Lundquist number ordering

Suppose that Lundquist number is sufficiently large that the final term in Eq. (22) is completely dominant. In other words, suppose that ion inertia can be entirely neglected in the vorticity equation. It follows that

$$[J,\psi] = 0, \quad (35)$$

i.e., the toroidal current density in the island region must be a magnetic flux-surface function (otherwise, the plasma would not be in force balance).

G. Rutherford ordering

Let us write

$$J(X,\zeta) = J_{\rm eq} + \delta J(X,\zeta), \quad (36)$$

$$\hat{T}(X,\zeta) = 1 - \left(\frac{w}{L_T}\right)\delta T(X,\zeta), \quad (37)$$

where

$$J_{\rm eq} = \frac{2}{s_s} - 1. \quad (38)$$

It follows that

$$\delta T(X,\zeta)|_{\lim|X|\to\infty} = X. \quad (39)$$

The so-called *Rutherford ordering*

$$|\delta J| \ll 1, \quad (40)$$

plays a crucial role in the analysis presented in this paper. In the absence of island asymmetry, this ordering is equivalent to the well-known *constant-ψ approximation*.[6] The purpose of the ordering is to simplify the simultaneous solution of Eqs. (24) and (35). Indeed, it can be seen that these equations yield

$$[J,\psi] = [\delta J,\psi], \quad (41)$$

$$\partial_X^2 \psi = 1 - \delta J, \quad (42)$$

which, with the aid of Eq. (40), reduces to the completely uncoupled (and, thus, easily solvable) pair of equations

$$\delta J = \delta J(\psi), \quad (43)$$

$$\partial_X^2 \psi \simeq 1. \quad (44)$$

Now, we know, from standard plasma theory, that[3]

$$\hat{\eta}(\hat{T}) = \hat{T}^{-3/2}. \quad (45)$$

Furthermore, it is assumed that ψ, δT, s_s, ∂_X, $\partial_\zeta \sim O(1)$, and w/L_T, $\alpha_b\,L_s/L_T$, ϕ, U, $\mathcal{E}$, $\Delta' w \sim \mathcal{O}(\delta J)$, and $\partial/\partial t \sim \mathcal{O}[\delta J/(w/r_s)^2\,\tau_R]$. Equations (21), (23), (25), and (34) yield

$$\tau_R \frac{\partial}{\partial t}\left[\left(\frac{w}{r_s}\right)^2 \psi\right] \simeq [\phi,\psi] + \alpha_b\,\frac{L_s}{L_T}(\partial_X \delta T - 1) - \frac{3}{2}\,\frac{w}{L_T}\left(\frac{2}{s_s} - 1\right)\delta T - \delta J, \quad (46)$$

$$0 \simeq \left(\frac{w}{w_c}\right)^4 [[\delta T, \psi], \psi] + \partial_X^2 \delta T, \tag{47}$$

$$\Delta' w = -2 \int_{-\infty}^{\infty} \oint \delta J \cos\zeta \, dX \, \frac{d\zeta}{2\pi}. \tag{48}$$

Note that the Rutherford ordering (40) implies that [see Eq. (48)]

$$|\Delta' w| \ll 1, \tag{49}$$

but not that $|\Delta' r_s| \ll 1$ (assuming that $w \ll r_s$). Furthermore, the large Lundquist number ordering holds provided

$$\frac{w}{r_s} \gg \left(|\Delta' w|\right)^{1/6} S^{-1/3}, \tag{50}$$

which is easily satisfied in a high-temperature tokamak plasma. Finally, the neglect of the ohmic heating term in Eq. (47) is valid provided

$$\frac{\tau_E}{\beta \tau_R} \left(\frac{L_T}{L_s}\right)^2 \delta J^3 \ll 1, \tag{51}$$

which is easily satisfied in the Rutherford ordering (especially, since it is generally the case that $\tau_E \ll \tau_R$ and $\beta^{-1} (L_T/L_s)^2 \leq 1$). [Any temperature peaking inside the island due to the background ohmic heating can be shown to be negligible provided that $(\tau_E/\beta\tau_R)(L_T/L_s)^2 \delta J^2 \ll 1$, which is easily satisfied in the Rutherford ordering.]

H. Flux-surface average operator

Let us define a magnetic *flux-surface average operator*, $\langle \cdots \rangle$, such that

$$\langle [A, \psi] \rangle = 0, \tag{52}$$

for arbitrary $A(X, \zeta)$.

I. Reduced resistive-MHD evolution equations

The flux-surface average of Eq. (46) can be combined with Eqs. (39), (43), (44), (47), and (48) to give the following complete set of equations that govern the resistive evolution of the magnetic island chain:

$$\partial_X^2 \psi = 1, \tag{53}$$

$$0 = \left(\frac{w}{w_c}\right)^4 [[\delta T, \psi], \psi] + \partial_X^2 \delta T, \tag{54}$$

$$\delta T(X, \zeta)|_{\lim |X| \to \infty} = X, \tag{55}$$

$$\delta J(\psi) = -\frac{\tau_R}{\langle 1 \rangle} \frac{\partial}{\partial t} \left[\left\langle \left(\frac{w}{r_s}\right)^2 \psi \right\rangle \right] + \alpha_b \frac{L_s}{L_T} \left(\frac{\langle \partial_X \delta T \rangle}{\langle 1 \rangle} - 1 \right) - \frac{3}{2} \frac{w}{L_T} \left(\frac{2}{s_s} - 1 \right) \frac{\langle \delta T \rangle}{\langle 1 \rangle}, \tag{56}$$

$$\Delta' w = -2 \int_{-\infty}^{\infty} \oint \delta J(\psi) \cos\zeta \, dX \, \frac{d\zeta}{2\pi}. \tag{57}$$

III. RADIALLY ASYMMETRIC MAGNETIC ISLAND CHAIN

A. Model magnetic flux surfaces

Let us adopt the following solution of Eq. (53):

$$\psi(X, \zeta) = \Omega(X, \zeta), \tag{58}$$

where

$$\Omega(X, \zeta) \equiv \frac{1}{2} X^2 + \cos(\zeta - \delta^2 \sin\zeta) - \sqrt{2}\, \delta X \cos\zeta + \delta^2 \cos^2\zeta + \mathcal{O}(\Delta' w). \tag{59}$$

As illustrated in Figs. 1–3, the magnetic flux-surfaces (i.e., the contours of Ω) in the vicinity of the rational surface [i.e., for $|X| \sim \mathcal{O}(1)$] map out an asymmetric (with respect to $X = 0$) magnetic island chain whose O-points lie at $\zeta = \pi$, $X = -\sqrt{2}\,\delta$, and $\Omega = -1$, and whose X-points lie at $\zeta = 0, 2\pi$, $X = +\sqrt{2}\,\delta$, and $\Omega = +1$. The magnetic separatrix corresponds to $\Omega = +1$, the region inside the separatrix to $-1 \leq \Omega < 1$, and the region outside the separatrix to $\Omega > 1$. The full radial island width (in X) is 4.

Note that the model magnetic flux surfaces specified in Eq. (59) satisfy the fundamental force balance constraint

$$[\partial_X^2 \Omega, \Omega] = 0. \tag{60}$$

[See Eqs. (35), (41), (42), and (58).] This is not the case for the model surfaces adopted in Refs. 15–17.

The first term on the right-hand side of Eq. (59) emanates from the unperturbed (by the tearing mode) plasma equilibrium, whereas the remaining terms emanate from the previously mentioned linear ideal-MHD solution in the outer region. In particular, the third term on the right-hand side, which governs the island asymmetry, originates from the mean radial gradient in the $\cos\zeta$ component of the linear ideal-MHD eigenfunction at the rational surface. Note that,

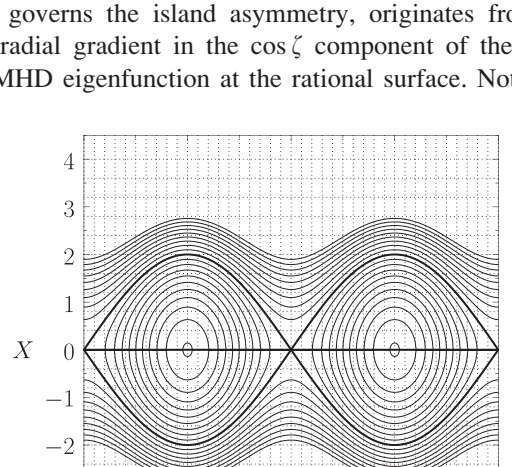

FIG. 1. The thin solid curves show contours of $\Omega(X, \zeta)$ evaluated for $\delta = 0.0$. The thick solid curves show the magnetic separatrix (upper and lower curves) and the contour $Y = 0$ (middle curve). The horizontal dotted lines show equally spaced contours of Y, whereas the vertical dotted lines show equally spaced contours of ξ.

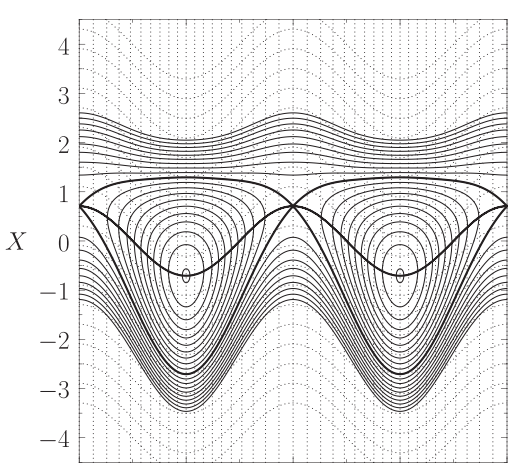

FIG. 2. The thin solid curves show contours of $\Omega(X,\zeta)$ evaluated for $\delta = 0.5$. The thick solid curves show the magnetic separatrix (upper and lower curves) and the contour $Y = 0$ (middle curve). The curved dotted lines show equally spaced contours of Y, whereas the vertical dotted lines show equally spaced contours of ξ.

as a consequence of the Rutherford ordering (i.e., $|\Delta' w| \ll 1$), which plays a central role in our analysis, the jump in the radial gradient of the $\cos\zeta$ component across the rational surface, that ultimately yields the Δ' parameter [see Eqs. (24), (36), and (57)], is much smaller than the mean radial gradient [assuming that $\delta \sim \mathcal{O}(1)$]. Hence, to lowest order, we can neglect this jump when calculating the island structure in the vicinity of the rational surface. Unfortunately, the Rutherford ordering necessarily restricts our analysis to island chains in which the radial shift of the O-points is equal and opposite to that of the X-points. To be more exact, the difference between the magnitudes of the shifts divided by the island width must be, at most, $\mathcal{O}(\Delta' w)$.

The island asymmetry is governed by the dimensionless parameter δ. If $\delta > 0$ then the island O-points are displaced radially inward (with respect to the unperturbed rational surface), whereas the X-points are displaced radially outward an equal distance. The opposite is the case if $\delta < 0$. Generally speaking, we expect $\delta > 0$ for low mode-number tearing modes in tokamak plasmas (because the ideal-MHD eigenfunctions for such modes tend to attain their maximum amplitudes inside the rational surface; see Fig. 2 in Ref. 17). Note that if δ exceeds the critical value unity then the X-points bifurcate, and it is no longer possible to analyze the resistive evolution of the resulting island chain using a variant of standard Rutherford island theory.[7] Hence, we shall only consider the case $0 \leq \delta < 1$.

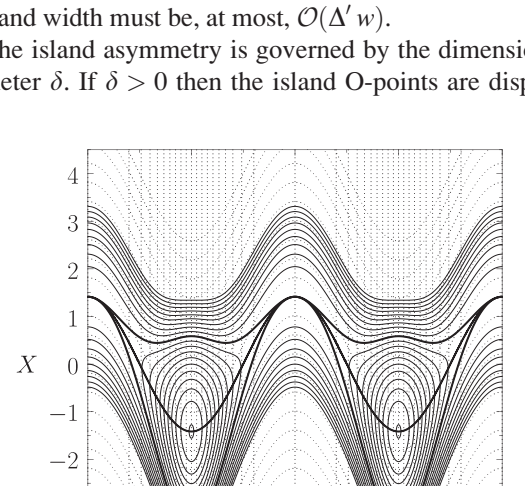

FIG. 3. The thin solid curves show contours of $\Omega(X,\zeta)$ evaluated for $\delta = 1.0$. The thick solid curves show the magnetic separatrix (upper and lower curves) and the contour $Y = 0$ (middle curve). The curved dotted lines show equally spaced contours of Y, whereas the vertical dotted lines show equally spaced contours of ξ.

In the region outside the magnetic separatrix, we can write

$$\Omega(X,\zeta) = \frac{1}{2}(X - \Xi)^2, \tag{61}$$

where $\Xi(X,\zeta)$ is the radial displacement (normalized to w) of magnetic flux-surfaces induced by the tearing perturbation. It follows that

$$\Xi(X,\zeta) \simeq -\frac{[\Omega(X,\zeta) - X^2/2]}{X} = \sqrt{2}\,\delta\,\cos\zeta - \frac{\cos(\zeta - \delta^2\,\sin\zeta) + \delta^2\,\cos^2\zeta}{X}. \tag{62}$$

Note the radial flux-surface displacement asymptotes to zero in the outer region (i.e., $|X| \gg 1$) for the case of a symmetric island chain (i.e., $\delta = 0$). On the other hand, the displacement asymptotes to a finite helical value for the case of an asymmetric island chain (i.e., $\delta > 0$).

B. Harmonic decomposition

Let us write

$$\Omega(X,\zeta) = \sum_{n=0,\infty} \Omega_n(X)\,\cos\zeta. \tag{63}$$

It follows that

$$\Omega_0(X) = \oint \Omega(X,\zeta)\,\frac{d\zeta}{2\pi}, \tag{64}$$

$$\Omega_{n>0}(X) = 2\oint \Omega(X,\zeta)\cos(n\,\zeta)\,\frac{d\zeta}{2\pi}. \tag{65}$$

Now,[25,26]

$$J_n(\delta^2) = \oint \cos\left(n\,\zeta - \delta^2\,\sin\zeta\right)\frac{d\zeta}{2\pi}, \tag{66}$$

$$J_{-n}(\delta^2) = (-1)^n\,J_n(\delta^2), \tag{67}$$

where the $J_n(x)$ are standard Bessel functions. Hence, Eqs. (59), (64), and (65) yield

$$\Omega_0(X) = \frac{1}{2}\,X^2 + \frac{\delta^2}{2} + J_1(\delta^2), \tag{68}$$

$$\Omega_{n>0}(X) = -\sqrt{2}\,\delta\,X\,\delta_{n,1} + \frac{\delta^2}{2}\,\delta_{n,2} + (-1)^{n-1}\,J_{n-1}(\delta^2) + J_{n+1}(\delta^2). \tag{69}$$

The first few Fourier harmonics of $\Omega(0,\zeta)$ are plotted as a function of the asymmetry parameter, δ, in Fig. 4. It can be seen that the $n=0$ and $n=1$ harmonics are dominant, even in the limit that $\delta \rightarrow 1$. (This is consistent with Rutherford's original analysis, which mandates that the non-axisymmetric component of ψ should be dominated by a single Fourier component.) Indeed, when $\delta \ll 1$, we obtain

$$\Omega(X,\zeta) = \frac{1}{2}X^2 + \left(1-\sqrt{2}\,\delta\,X\right)\cos\zeta + \delta^2 + \mathcal{O}(\delta^4). \quad (70)$$

C. Coordinate transformation

Let us define the new coordinates

$$Y = X - \sqrt{2}\,\delta\,\cos\zeta, \quad (71)$$

$$\xi = \zeta - \delta^2\,\sin\zeta. \quad (72)$$

When expressed in terms of these coordinates, the magnetic flux-function (59) reduces to the simple form

$$\Omega(Y,\xi) = \frac{1}{2}Y^2 + \cos\xi. \quad (73)$$

Thus, as illustrated in Fig. 5, irrespective of the value of the asymmetry parameter, δ, when plotted in Y, ξ space, the magnetic flux-surfaces map out a symmetric (with respect to $Y=0$) island chain whose O-points lie at $\xi=\pi$, $Y=0$, and $\Omega=-1$, and whose X-points lie at $\xi=0,2\pi$, $Y=0$, and $\Omega=+1$. As before, the magnetic separatrix corresponds to $\Omega=+1$, the region inside the separatrix to $-1\leq\Omega<1$, and the region outside the separatrix to $\Omega>1$. Moreover, the full radial island width (in Y) is still 4.

Because Eq. (72) has the same form as *Kepler's equation*, its inversion is very well known[25]

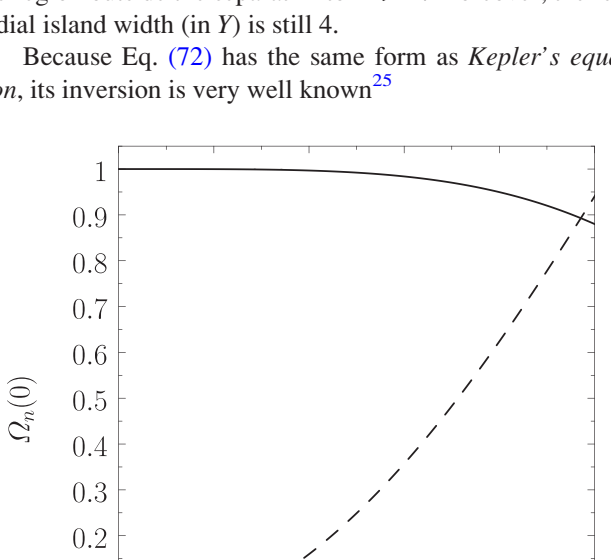

FIG. 4. The first few Fourier harmonics of $\Omega(0,\zeta)$ plotted as a function of the asymmetry parameter, δ. The dashed, solid, long-dashed, dash-dotted, and long-dash-dotted curves show $\Omega_0(0)$, $\Omega_1(0)$, $\Omega_2(0)$, $\Omega_3(0)$, and $\Omega_4(0)$, respectively.

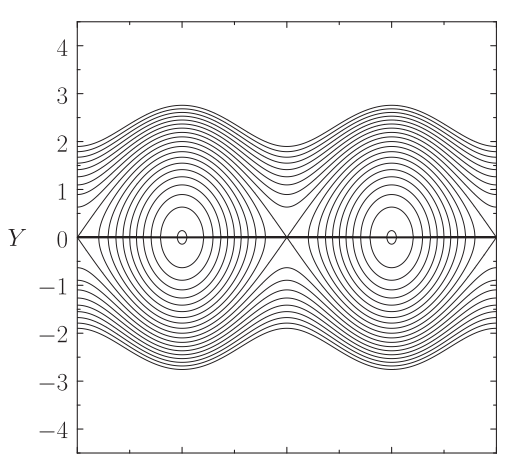

FIG. 5. The thin solid curves show contours of $\Omega(Y,\xi)$ evaluated for arbitrary δ. The thick solid line shows the contour $Y=0$.

$$\cos\zeta = -\frac{\delta^2}{2} + \sum_{n=1,\infty}\left[\frac{J_{n-1}(n\,\delta^2)-J_{n+1}(n\,\delta^2)}{n}\right]\cos(n\,\xi), \quad (74)$$

$$\cos(m\,\zeta) = m\sum_{n=1,\infty}\left[\frac{J_{n-m}(n\,\delta^2)-J_{n+m}(n\,\delta^2)}{n}\right]\cos(n\,\xi), \quad (75)$$

$$\sin\zeta = \frac{2}{\delta^2}\sum_{n=1,\infty}\left[\frac{J_n(n\,\delta^2)}{n}\right]\sin(n\,\xi), \quad (76)$$

$$\zeta = \xi + 2\sum_{n=1,\infty}\left[\frac{J_n(n\,\delta^2)}{n}\right]\sin(n\,\xi), \quad (77)$$

for $m>1$. We can also write

$$\cos\xi = J_1(\delta^2) + \sum_{n=1,\infty}\left[(-1)^{n-1}J_{n-1}(\delta^2)+J_{n+1}(\delta^2)\right]\cos(n\,\zeta), \quad (78)$$

$$\sin\xi = \sum_{n=1,\infty}\left[(-1)^{n-1}J_{n-1}(\delta^2)-J_{n+1}(\delta^2)\right]\sin(n\,\zeta), \quad (79)$$

where use has been made of Eqs. (66), (67), and (72). Finally, it is helpful to define

$$\sigma(\xi) \equiv \frac{d\zeta}{d\xi} = 1 + 2\sum_{n=1,\infty}J_n(n\,\delta^2)\cos(n\,\xi). \quad (80)$$

D. Flux coordinate system

Let us introduce the flux coordinate system s, Ω, ξ, where

$$Y(s,\Omega,\xi) = s\sqrt{2\,(\Omega-\cos\xi)}. \quad (81)$$

It follows that $s=+1$ for $Y>0$ (which corresponds to $X>\sqrt{2}\,\delta\,\cos\zeta$), and $s=-1$ for $Y<0$ (which corresponds to $X<\sqrt{2}\,\delta\,\cos\zeta$). Now,

$$\partial_X = \partial_Y = Y(s,\Omega,\xi)\,\partial_\Omega, \quad (82)$$

and

$$\frac{\partial(X,\zeta)}{\partial(\Omega,\xi)} = \frac{\sigma(\xi)}{Y(s,\Omega,\xi)}, \tag{83}$$

where $\partial_X \equiv \partial/\partial X|_\zeta$, $\partial_Y \equiv \partial/\partial Y|_\zeta$, and $\partial_\Omega \equiv \partial/\partial\Omega|_\xi$. Hence,

$$dX\, d\zeta = \frac{\sigma(\xi)}{Y(s,\Omega,\xi)}\, d\Omega\, d\xi, \tag{84}$$

$$[A,B] = \partial_Y A\, \partial_\zeta B - \partial_\zeta A\, \partial_Y B = \frac{Y(s,\Omega,\xi)}{\sigma(\xi)}\,(\partial_\Omega A\, \partial_\xi B - \partial_\xi A\, \partial_\Omega B), \tag{85}$$

$$[A,\Omega] = -\frac{Y(s,\Omega,\xi)}{\sigma(\xi)}\,\partial_\xi A. \tag{86}$$

Here, $\partial_\zeta \equiv \partial/\partial\zeta|_Y$, and $\partial_\xi \equiv \partial/\partial\xi|_\Omega$.

E. Flux-surface average operator

The flux-surface average operator, $\langle\cdots\rangle$, is defined in Eq. (52). Thus, it follows from Eqs. (58), (81), and (86) that

$$\langle A\rangle = \int_{\xi_0}^{2\pi-\xi_0} \frac{\sigma(\xi)\, A_+(\Omega,\xi)}{\sqrt{2\,(\Omega-\cos\xi)}}\,\frac{d\xi}{2\pi}, \tag{87}$$

for $-1 \le \Omega \le 1$, and

$$\langle A\rangle = \int_0^{2\pi} \frac{\sigma(\xi)\, A(s,\Omega,\xi)}{\sqrt{2\,(\Omega-\cos\xi)}}\,\frac{d\xi}{2\pi}, \tag{88}$$

for $\Omega > 1$. Here, $\xi_0 = \cos^{-1}(\Omega)$, and

$$A_\pm(\Omega,\xi) = \frac{1}{2}[A(+1,\Omega,\xi) \pm A(-1,\Omega,\xi)]. \tag{89}$$

More generally,

$$A_\pm(Y,\zeta) = \frac{1}{2}[A(Y,\zeta) \pm A(-Y,\zeta)]. \tag{90}$$

F. Rutherford island width evolution equation

Equations (43), (57), (58), (81), (84), and (87)–(89) imply that

$$\Delta' w = -4\int_{-1}^{\infty} \delta J_+(\Omega)\,\langle\cos\zeta\rangle\, d\Omega. \tag{91}$$

However, it follows from Eqs. (56), (58), and (87)–(90) that

$$\delta J_+(\Omega) = -\frac{\tau_R}{\langle 1\rangle}\frac{\partial}{\partial t}\left[\left\langle\left(\frac{w}{r_s}\right)^2\Omega\right\rangle_+\right] + \alpha_b\frac{L_s}{L_T}\left(\frac{d_\Omega\langle|Y|\,\delta T_-\rangle}{\langle 1\rangle} - 1\right) - \frac{3}{2}\frac{w}{L_T}\left(\frac{2}{s_s}-1\right)\frac{\langle\delta T_+\rangle}{\langle 1\rangle}. \tag{92}$$

Here, $|Y| = s\,Y$, $d_\Omega \equiv d/d\Omega$, and use has been made of the easily demonstrated result $\langle\partial_X \delta T\rangle_+ = \langle Y\,\partial_\Omega \delta T\rangle_+ = d_\Omega\langle|Y|\,\delta T_-\rangle$. Now, according to Eq. (59)

$$w^2\,\Omega = -\frac{1}{2}\,x^2 + w^2\,\cos\Big(\zeta - w^2\,\hat\delta^2\,\sin\zeta\Big) - \sqrt{2}\,w^2\,\hat\delta\,x\,\cos\zeta + \frac{1}{2}\,w^4\,\hat\delta^2\,[1+\cos(2\,\zeta)], \tag{93}$$

where $\hat\delta = \delta/w$ is assumed to be time independent (because, to lowest order, the mean logarithmic radial gradient in the ideal-MHD eigenfunction at the rational surface is independent of the island width). Thus,

$$\left|\frac{\partial\,(w^2\,\Omega)}{\partial t}\right|_{x,\zeta} = 2\,w\,\frac{dw}{dt}\big(\cos\xi + \delta^2\,\sin\xi\,\sin\zeta - \sqrt{2}\,\delta\,X\,\cos\zeta + 2\,\delta^2\,\cos^2\zeta\big), \tag{94}$$

where use has been made of Eq. (72). From Eq. (71), the previous equation becomes

$$\left|\frac{\partial\,(w^2\,\Omega)}{\partial t}\right|_{x,\zeta} = 2\,w\,\frac{dw}{dt}\big(\cos\xi + \delta^2\,\sin\xi\,\sin\zeta - \sqrt{2}\,\delta\,Y\,\cos\zeta\big). \tag{95}$$

Hence, Eqs. (91) and (92) yield the so-called *Rutherford island width evolution equation*[7]

$$G_1\,\tau_R\,\frac{d}{dt}\left(\frac{W}{r_s}\right) = \Delta'\,r_s + G_2\,\alpha_b\,\frac{L_s}{L_T}\,\frac{r_s}{W} + G_3\,\frac{r_s}{L_T}\left(\frac{2}{s_s}-1\right), \tag{96}$$

where

$$G_1 = 2\int_{-1}^{\infty}\frac{\big(\langle\cos\xi\rangle + \delta^2\,\langle\sin\xi\,\sin\zeta\rangle\big)\,\langle\cos\zeta\rangle}{\langle 1\rangle}\,d\Omega, \tag{97}$$

$$G_2 = 16\int_{-1}^{\infty}\frac{\langle\partial_Y\delta T_-\rangle\,\langle\cos\zeta\rangle}{\langle 1\rangle}\,d\Omega = 16\int_{-1}^{\infty}\frac{d_\Omega\langle|Y|\,\delta T_-\rangle\,\langle\cos\zeta\rangle}{\langle 1\rangle}\,d\Omega, \tag{98}$$

$$G_3 = -6\int_{-1}^{\infty}\frac{\langle\delta T_+\rangle\,\langle\cos\zeta\rangle}{\langle 1\rangle}\,d\Omega. \tag{99}$$

Here, $W = 4\,w$ is the full island width. The first term on the right-hand side of Eq. (96) is the usual drive that originates from equilibrium current gradients in the outer region. The second term is a drive that emanates from changes in the non-inductive bootstrap current density in the inner region induced by localized temperature perturbations (which modify the plasma pressure gradient).[13] The third term is a drive that emanates from changes in the inductive current density induced by localized temperature perturbations (which modify the plasma electrical conductivity).[10,17] Here, use has been made of the easily proved result $\int_{-1}^{\infty}\langle\cos\zeta\rangle\,d\Omega = 0$.

IV. NARROW-ISLAND LIMIT

A. Introduction

Consider the so-called *narrow-island limit*[4]

$$w \ll w_c, \tag{100}$$

in which the parallel thermal conductivity is not sufficiently large to force the temperature profile to be a magnetic flux-surface function in the inner region.

B. Solution of temperature profile equation

The temperature profile in the inner region is determined from the solution of Eq. (54), which can be written

$$\left(\frac{w}{w_c}\right)^4 (Y\,\partial_\zeta + S\,\partial_Y)^2 \delta T + \partial_Y^2 \delta T = 0, \tag{101}$$

where

$$S(\zeta) = -d_\zeta C, \tag{102}$$

$$C(\zeta) = \cos(\zeta - \delta^2\,\sin\zeta). \tag{103}$$

Here, $d_\zeta \equiv d/d\zeta$, and use has been made of Eqs. (58), (72), (73), (82), and (85).

Let

$$Z = \frac{w}{w_c}\,Y. \tag{104}$$

Equation (101) reduces to

$$\left[Z\,\partial_\zeta + \left(\frac{w}{w_c}\right)^2 S\,\partial_Z\right]^2 \delta T + \partial_Z^2 \delta T = 0, \tag{105}$$

where $\partial_Z \equiv \partial/\partial_Z|_\zeta$. This can be written

$$Z^2\,\partial_\zeta^2 \delta T + \partial_Z^2 \delta T - \left(\frac{w}{w_c}\right)^2 (d_\zeta C\,\partial_\zeta \delta T + 2\,d_\zeta C\,Z\,\partial_{\zeta,Z}^2 \delta T + d_\zeta^2 C\,Z\,\partial_Z \delta T\Big) = \mathcal{O}\left(\frac{w}{w_c}\right)^4. \tag{106}$$

Let

$$\delta T(Z,\zeta) = \delta T_0(Z) + 2\sum_{n=1,\infty} \delta T_n(Z)\,\cos(n\,\zeta). \tag{107}$$

It follows that

$$d_Z^2 \delta T_0 \simeq 0, \tag{108}$$

$$d_Z^2 \delta T_n - n^2\,Z^2\,\delta T_n \simeq -\frac{1}{2}\left(\frac{w}{w_c}\right)^2 n^2 \Big[(-1)^{n-1} J_{n-1}(\delta^2) + J_{n+1}(\delta^2)\Big] Z\,d_Z \delta T_0, \tag{109}$$

for $n > 0$. Here, use has been made of Eqs. (66) and (67). The previous two equations are accurate to $\mathcal{O}(w/w_c)^2$.

The solution of Eq. (108) that satisfies the boundary condition (55) is

$$\delta T_0 = \frac{w_c}{w}\,Z, \tag{110}$$

where use has been made of Eqs. (71) and (104). Hence, Eq. (109) yields

$$d_Z^2 \delta T_n - n^2\,Z^2\,\delta T_n \simeq -\frac{1}{2}\,\frac{w}{w_c}\,n^2 \Big[(-1)^{n-1} J_{n-1}(\delta^2) + J_{n+1}(\delta^2)\Big] Z. \tag{111}$$

Physically acceptable solutions of the previous equation are such that $\delta T_n(Z)$ and its first derivative are continuous, and $\delta T_n(Z)$ is well behaved as $|Z| \to \infty$. Thus, we deduce that

$$\delta T_+(Y,\zeta) = 0, \tag{112}$$

$$\delta T_-(Y,\zeta) = Y + \sum_{n=1,\infty} \frac{\sqrt{2\,n}}{4}\,\frac{w}{w_c}\Big[(-1)^{n-1} J_{n-1}(\delta^2) + J_{n+1}(\delta^2)\Big] f\left(\sqrt{2\,n}\,\frac{w}{w_c}\,Y\right)\cos(n\,\zeta), \tag{113}$$

where $f(p)$ is the solution of

$$\frac{d^2 f}{dp^2} - \frac{1}{4}\,p^2 f = -p, \tag{114}$$

that satisfies $f(0) = 0$, and $f \to 0$ as $|p| \to \infty$. This solution is shown in Fig. 6. Note that $f(p) \simeq 1.198\,p$ for $|p| \ll 1$, and $f(p) \simeq 4/p$ for $|p| \gg 1$.

In the vicinity of the magnetic separatrix [i.e., $|Z| \sim \mathcal{O}(1)$], Eqs. (112) and (113) yield

$$\delta T \simeq Y = X - \sqrt{2}\,\delta\,\cos\zeta, \tag{115}$$

where use has been made of Eq. (71). On the other hand, far from the magnetic separatrix (i.e., $|Z| \gg 1$), the same equations imply that

$$\delta T \simeq Y + \frac{\cos\xi - J_1(\delta^2)}{Y}, \tag{116}$$

where Eq. (78) has been employed. However,

$$Y \simeq s\left(\sqrt{2\,\Omega} - \frac{\cos\xi}{\sqrt{2\,\Omega}}\right), \tag{117}$$

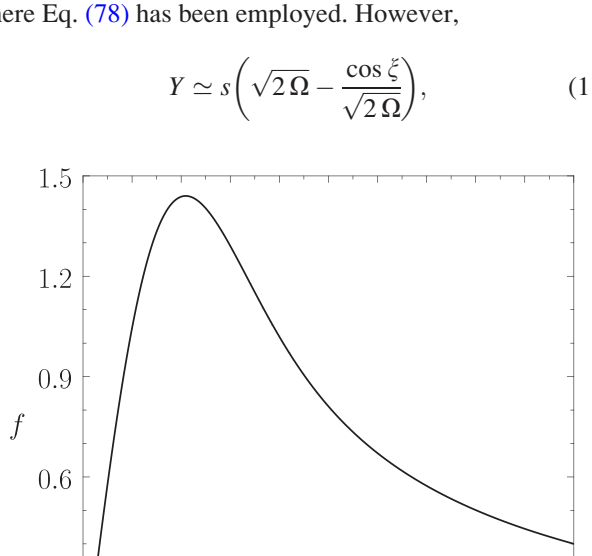

FIG. 6. The function $f(p)$.

when $|\Omega| \gg 1$, where use has been made of Eq. (81). Thus, Eq. (116) gives

$$\delta T \simeq s\left[\sqrt{2\,\Omega} - \frac{J_1(\delta^2)}{\sqrt{2\,\Omega}}\right], \tag{118}$$

in the limit $\Omega \gg 1$. We conclude that the temperature profile asymptotes to an odd (in Y) flux-surface function in the outer region. Furthermore, the fact that the magnetic flux-surfaces have a finite helical displacement in the outer region (see Sec. III A) causes the temperature contours to exhibit a finite helical displacement in the immediate vicinity of the island separatrix [see Eq. (115)]. (Here, we are assuming that $\delta > 0$.) The only case in which this argument does not hold is the completely unrealistic one in which the ratio $\kappa_\parallel/\kappa_\perp$ is so small that the inequality $w_c \ll r_s$ is not satisfied [see Eq. (33)]. It follows that, for the case of a radially asymmetric island chain, it is not correct to assume that $\delta T \simeq \delta T(X)$ [which implies that $\eta = \eta(X)$] in the narrow-island limit.[10] On the other hand, this assumption would be reasonable for the case of a symmetric island chain. This point is further illustrated in Figs. 7 and 8, which show contours of δT in the vicinity of a symmetric and an asymmetric island chain, respectively, in the narrow-island limit. In the former case, it is approximately true that $\delta T = \delta T(X)$, whereas this is clearly not true in the latter case.

C. Rutherford island width evolution equation

The analysis of the Sec. IV B reveals that

$$\delta T_+ = 0, \tag{119}$$

in the narrow-island limit. In other words, the temperature profile in the vicinity of the magnetic island chain is an odd function of Y. This result is general and ultimately derives from the fact that the temperature profile equation, (101), is invariant under the transformation $Y \Longrightarrow -Y$ [i.e., there is

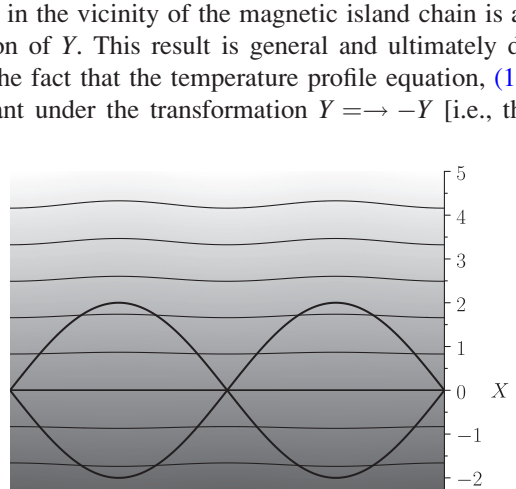

FIG. 7. Temperature contours in the vicinity of a symmetric magnetic island chain in the narrow-island limit. The calculation parameters are $\delta = 0.0$, $w/w_c = 0.2$, and $N = 40$. The thick solid curve indicates the position of the magnetic separatrix. Note that the temperature contours do not coincide with magnetic flux-surfaces. However, it is approximately true that $\delta T = \delta T(X)$.

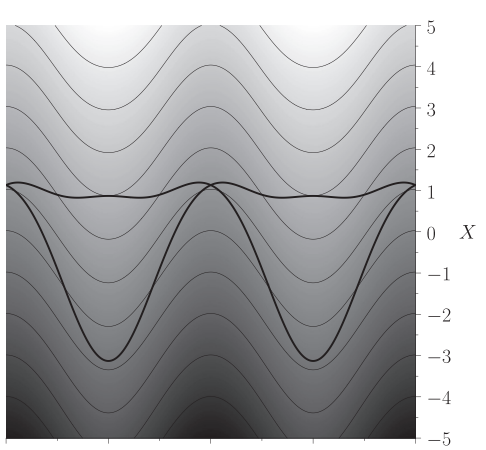

FIG. 8. Temperature contours in the vicinity of an asymmetric magnetic island chain in the narrow-island limit. The calculation parameters are $\delta = 0.8$, $w/w_c = 0.2$, and $N = 40$. The thick solid curve indicates the position of the magnetic separatrix. Note that the temperature contours do not coincide with magnetic flux-surfaces. Furthermore, it is not true that $\delta T = \delta T(X)$, even to a first approximation.

no coupling between even- and odd-parity (in Y) solutions of this equation]. Equations (99) and (119) imply that

$$G_3 = 0. \tag{120}$$

In other words, the third term on the right-hand side of the Rutherford island equation, (96), which emanates from temperature-induced perturbations to the inductive current density in the inner region, is zero by symmetry. Note that this result holds even in the presence of finite island asymmetry (i.e., $\delta > 0$). The result $G_3 = 0$, obtained in this paper, differs from that of Ref. 10, which claims that $G_3 > 0$ (assuming that $\delta > 0$) in the narrow-island limit. This disagreement can be attributed to the fact that Ref. 10 assumes that $\delta T = \delta T(X)$ in the narrow-island limit. However, as is discussed in Sec. IV B, this assumption is not appropriate to the case of an asymmetric island chain.

Making use of Eqs. (98), (113), and (120), the Rutherford island width evolution equation in the narrow-island limit reduces to[4]

$$G_1\,\tau_R\,\frac{d}{dt}\left(\frac{W}{r_s}\right) = \Delta'\,r_s + G_2'\,\alpha_b\,\frac{L_s}{L_T}\,\frac{W\,r_s}{W_c^2}, \tag{121}$$

where $W_c = 4\,w_c$, and

$$G_2' = 8 f'(0)\sum_{n=1,\infty} n\left[(-1)^{n-1}\,J_{n-1}(\delta^2) + J_{n+1}(\delta^2)\right] \times \int_{-1}^{\infty} \frac{\langle\cos(n\,\zeta)\rangle\,\langle\cos\zeta\rangle}{\langle 1\rangle}\,d\Omega. \tag{122}$$

Here, $f'(0) \equiv (df/dp)_{p=0} = 1.198$. Figure 9 shows G_1 and G_2', evaluated as functions of the island asymmetry parameter, δ, by means of the analysis outlined in the Appendix. It can be seen that $G_1 > 0$ is virtually independent of island asymmetry.[16] It can also be seen that $G_2' > 0$, which implies that the perturbed bootstrap current has a destabilizing effect on the tearing perturbation in the narrow-island limit.

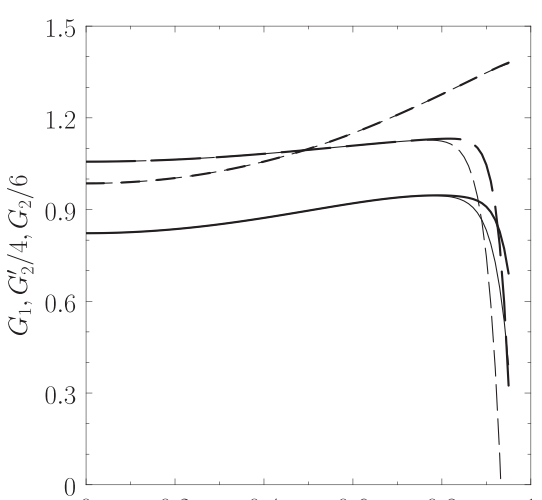

FIG. 9. The solid, short-dashed, and long-dashed curves show G_1, $G_2'/4$, and $G_2/6$, respectively, calculated as functions of the island asymmetry parameter, δ. The thick curves are calculated with $N = 15$, and the thin curves with $N = 10$.

Furthermore, G_2' exhibits a modest (i.e., about 40%) increase with increasing island asymmetry, indicating that asymmetry has a modest destabilizing effect in the narrow-island limit.

V. WIDE-ISLAND LIMIT

A. Introduction

Consider the so-called *wide-island limit*[4]

$$w \gg w_c, \tag{123}$$

in which the parallel thermal conductivity is sufficiently large to force the temperature profile to be a magnetic flux-surface function in the immediate vicinity of the magnetic separatrix.

B. Solution of temperature profile equation

The temperature profile in the inner region is determined from the solution of Eq. (54), which, in the limit $w/w_c \gg 1$, implies that

$$\delta T = \delta T(s, \Omega), \tag{124}$$

where use has been made of Eq. (58). The flux-surface average of Eq. (54) then reduces to

$$d_\Omega(\langle Y^2\rangle\, d_\Omega \delta T) = 0. \tag{125}$$

However, the only well-behaved (i.e., continuous, with a continuous first derivative) solution of the previous equation that is consistent with the boundary condition (55) (which implies that $\delta T \rightarrow s\sqrt{2\,\Omega}$ as $\Omega \rightarrow \infty$) is

$$\delta T_+(\Omega) = 0, \tag{126}$$

$$\delta T_-(\Omega) = \begin{cases} 0 & -1 \le \Omega \le 1 \\ \displaystyle\int_1^\Omega \frac{d\Omega'}{\langle Y^2\rangle(\Omega')} & \Omega > 1. \end{cases} \tag{127}$$

Figures 10 and 11 show contours of δT in the vicinity of a symmetric and an asymmetric island chain, respectively, in the wide-island limit. Note that the temperature profile is completely flattened inside the magnetic separatrix.

C. Rutherford island width evolution equation

The analysis of the Sec. V B reveals that

$$\delta T_+ = 0, \tag{128}$$

in the wide-island limit. In other words, the temperature profile in the vicinity of the magnetic island chain is an odd function of Y. This result is general, and ultimately derives from the fact that the temperature profile equation, (125), is invariant under the transformation $Y = \rightarrow -Y$ [i.e., there is no coupling between even- and odd-parity (in Y) solutions of this equation]. Equations (99) and (128) imply that

$$G_3 = 0. \tag{129}$$

In other words, the third term on the right-hand side of the Rutherford island equation, (96), which emanates from temperature-induced perturbations to the inductive current density in the inner region, is zero by symmetry. Note that this result holds even in the presence of finite island asymmetry (i.e., $\delta > 0$). The result $G_3 = 0$, obtained in this paper, differs from that of Ref. 17, which claims that $G_3 \neq 0$ in the wide-island limit. This disagreement may be due to the fact that, as explained in Secs. II G and III A, the analysis in this paper depends crucially on the ordering $|\Delta' w| \ll 1$, which implies that any radial asymmetry in the island chain is such that the radial shift of the O-points is equal and opposite to that of the X-points, or, to be more exact, that the difference between the magnitudes of the shifts divided by the island width is, at most, $\mathcal{O}(\Delta' w)$. Thus, if the calculation of Ref. 17 is actually finding a destabilizing effect that emanates from a large relative difference in the magnitudes of the radial shifts of the O- and X-points then this would not be captured by our analysis.

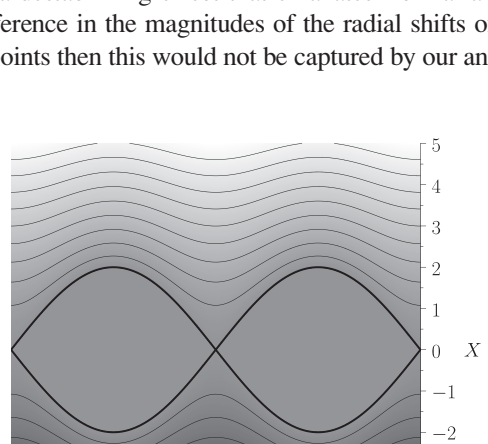

FIG. 10. Temperature contours in the vicinity of a symmetric magnetic island chain in the wide-island limit. The calculation parameters are $\delta = 0.0$. The thick solid curve indicates the position of the magnetic separatrix.

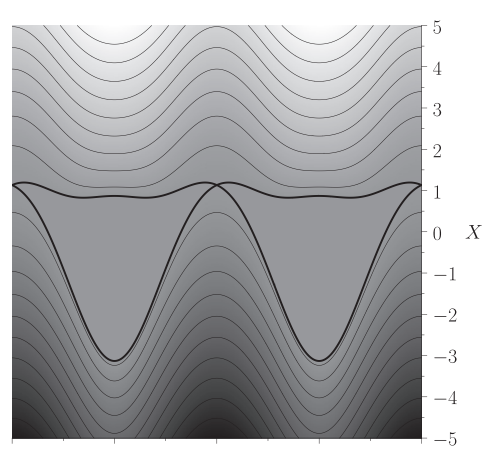

FIG. 11. Temperature contours in the vicinity of an asymmetric magnetic island chain in the wide-island limit. The calculation parameters are $\delta = 0.8$. The thick solid curve indicates the position of the magnetic separatrix.

Making use of Eqs. (98), (127), and (129), the Rutherford island width evolution equation in the wide-island limit reduces to

$$G_1\,\tau_R\,\frac{d}{dt}\left(\frac{W}{r_s}\right) = \Delta'\,r_s + G_2\,\alpha_b\,\frac{L_s}{L_T}\,\frac{r_s}{W}, \tag{130}$$

where

$$G_2 = 16\int_1^\infty \frac{\langle\cos\zeta\rangle}{\langle 1\rangle\,\langle Y^2\rangle}\,d\Omega. \tag{131}$$

Figure 9 shows G_2 evaluated as a function of the island asymmetry parameter, δ, by means of the analysis outlined in the Appendix. It can be seen that $G_2 > 0$, which implies that the perturbed bootstrap current has a destabilizing effect on the tearing perturbation in the wide-island limit. Note that G_2 is almost independent of the asymmetry parameter, indicating that radial asymmetry has virtually no effect on tearing mode stability in the wide-island limit.[16]

VI. SUMMARY AND DISCUSSION

In this paper, we have generalized the simple analysis of Rutherford[7] in order to incorporate radial island asymmetry into the nonlinear theory of tearing mode stability in a low-β, large aspect-ratio, quasi-cylindrical, tokamak plasma. For the sake of simplicity, we have concentrated on a particular (but fairly general) class of radially asymmetric island magnetic flux-surfaces that can all be mapped to the same symmetric flux-surfaces by means of a suitable coordinate transform. (See Sec. III.) Our analysis is restricted to the limits $|\Delta' w| \ll 1$ and $0 \leq |\delta| < 1$, where Δ' is the conventional tearing stability index, w is one-quarter of the full radial island width, the radial shift in the island X-points is $+(\sqrt{2}\,\delta - \alpha\,\Delta'\,w)\,w$, and that of the O-points is $-(\sqrt{2}\,\delta + \alpha\,\Delta'\,w)\,w$. Here, α is an (undetermined) positive $\mathcal{O}(1)$ constant. It follows that our analysis is restricted to cases in which the radial shift of the island X-points is (almost) equal and opposite to that of the O-points.

We find that the Rutherford island width evolution equation of a radially asymmetric island chain takes the general form

$$G_1\,\tau_R\,\frac{d}{dt}\left(\frac{W}{r_s}\right) = \Delta'\,r_s + \alpha_b\,\frac{L_s}{L_T}\,\frac{G_2\,G_2'\,W\,r_s}{G_2'\,W^2 + G_2\,W_c^2}. \tag{132}$$

(See Sections IV and V.) Here, τ_R is the resistive evolution time-scale at the rational surface, W the full radial island width, r_s the minor radius of the rational surface, L_s the magnetic shear-length at the rational surface, L_T the temperature gradient scale-length at the rational surface, and W_c the critical island width below which the temperature is no longer constrained to be a magnetic flux-surface function in the vicinity of the island chain. The dimensionless parameter α_b is defined in Eq. (31). Finally, the positive dimensionless constants G_1, G_2, and G_2' are evaluated as functions of the degree of island asymmetry in Fig. 9. It can be seen that G_1 and G_2 are virtually independent of island asymmetry, while G_2' exhibits a modest increase with increasing asymmetry. Note that Eq. (132) does not contain the higher-order saturation terms found in Refs. 8–10, because it was derived using a lowest-order asymptotic matching scheme. (See Sec. II B.) It follows that Eq. (132) is only valid for island widths significantly less than the final saturated width.

In principle, island asymmetry can affect tearing mode stability via one of the two mechanisms, both of which are associated with the modified temperature perturbation associated with the asymmetry. The first mechanism is via changes in the non-inductive bootstrap current density profile in the immediate vicinity of the island chain (this profile depends on the plasma pressure gradient, which, in turn, depends on the plasma temperature) and the second is via changes in the inductive current density profile (this profile depends on the plasma electrical conductivity, which, in turn, depends on the plasma temperature). The first mechanism gives rise to the second term on the right-hand side of Eq. (132). It follows that island asymmetry has a modest destabilizing effect (due to the increase in G_2' with increasing asymmetry) in the narrow-island limit, $W \ll W_c$, but has virtually no effect on stability in the wide-island limit, $W \gg W_c$ (because G_2 only depends very weakly on island asymmetry). On the other hand, the second mechanism gives rise to a term on the right-hand side of the Rutherford equation that turns out to be identically zero by symmetry (even for the case of an asymmetric island). In other words, the combination of radial island asymmetry (in which the radial shift of the X-points is almost equal and opposite to that of the O-points) and temperature-induced changes in the inductive current density profile in the island region has no effect on tearing mode stability.

In the Introduction, we mentioned the disagreement between the results appearing in Refs. 10 and 17. Reference 10 reports that, in the narrow-island limit, the aforementioned second mechanism gives rise to a significant destabilizing term in the Rutherford island width evolution equation that is proportional to the degree of radial asymmetry.

Furthermore, Ref. 17 reports that, in the wide-island limit, the second mechanism also gives rise to a significant destabilizing term in the Rutherford equation that is proportional to the radial asymmetry. However, Ref. 10 claims that the term in question is nonexistent in the wide-island limit. The existence, or otherwise, of the destabilizing term found in Ref. 17 is of particular importance because this term plays a crucial role in a recently developed theory of density limit disruptions in tokamak plasmas.[17–21] The main conclusion of this paper is that, in the limit $|\Delta' w| \ll 1$ and $0 \leq |\delta| < 1$, the term in question is nonexistent in both the narrow-island and the wide-island limits. The calculation in Ref. 10 (which is restricted to the limits $|\Delta' w| \ll 1$ and $|\delta| \ll 1$) is incorrect because it assumes that, in the narrow-island limit, $\eta = \eta(r)$ in the island region, which turns out not to be the case in the presence of island asymmetry. (See Sec. IV.) It is possible that the calculation in Ref. 17, which is of highly questionable validity because it does not respect the fundamental force-balance constraint $[J, \psi] = 0$ in the island region (see Sec. II F), is finding a destabilizing effect due to the difference in the magnitudes of the radial shifts in the island X- and O-points (this difference being proportional to $\Delta' w$). Thus, further research is needed to fully resolve the disagreement between the results appearing in Refs. 10 and 17.

ACKNOWLEDGMENTS

This research was funded by the U.S. Department of Energy under Contract No. DE-FG02-04ER-54742.

APPENDIX: CALCULATION OF FLUX-SURFACE AVERAGES

It is convenient to define the alternative flux-surface label, k, where $\Omega = 2\,k^2 - 1$. Thus, the island O-points corresponds to $k = 0$, the magnetic separatrix to $k = 1$, and $k \to \infty$ as $\Omega \to \infty$. It can be shown from Eqs. (87) and (88) that

$$\langle A \rangle = \int_{-\pi/2}^{\pi/2} \frac{\sigma(\xi)\, A_+(k,\theta)}{\sqrt{1 - k^2\, \sin^2\theta}}\, \frac{d\theta}{2\pi}, \tag{A1}$$

for $0 \leq k \leq 1$, where $\xi = 2\, \cos^{-1}(k\, \sin\theta)$. Likewise,

$$\langle A \rangle = \int_{-\pi/2}^{\pi/2} \frac{\sigma(\xi)\, A(s,k,\theta)}{\sqrt{k^2 - \sin^2\theta}}\, \frac{d\theta}{2\pi}, \tag{A2}$$

for $k > 1$, where $\xi = \pi - 2\,\theta$. Furthermore, from Eq. (80),

$$\sigma(\xi) = 1 + 2 \sum_{n=1,\infty} J_n(n\,\delta^2)\, \cos(n\,\xi). \tag{A3}$$

Let

$$C_n(k) = \begin{cases} \displaystyle\int_0^{\pi/2} \frac{\cos[2\,n\, \cos^{-1}(k\, \sin\theta)]}{\sqrt{1 - k^2\, \sin^2\theta}}\, d\theta & 0 \leq k \leq 1 \\ \displaystyle\int_0^{\pi/2} \frac{\cos[n\,(2\,\theta - \pi)]}{\sqrt{k^2 - \sin^2\theta}}\, d\theta & k > 1. \end{cases} \tag{A4}$$

Note that $C_{-n} = C_n$. It follows that

$$\langle \cos(m\,\xi) \rangle = \frac{1}{\pi} C_m(k) + \frac{1}{\pi} \sum_{n=1,\infty} J_n(n\,\delta^2)\, \big[C_{n-m}(k) + C_{n+m}(k)\big]. \tag{A5}$$

Moreover,

$$\langle \cos\zeta \rangle = -\frac{\delta^2}{2} \langle 1 \rangle + \sum_{n=1,\infty} \left[\frac{J_{n-1}(n\,\delta^2) - J_{n+1}(n\,\delta^2)}{n}\right] \langle \cos(n\,\xi) \rangle, \tag{A6}$$

$$\langle \cos(m\,\zeta) \rangle = m \sum_{n=1,\infty} \left[\frac{J_{n-m}(n\,\delta^2) - J_{n+m}(n\,\delta^2)}{n}\right] \langle \cos(n\,\xi) \rangle, \tag{A7}$$

$$\delta^2\, \langle \sin\xi\, \sin\zeta \rangle = \sum_{n=1,\infty} \left[\frac{J_n(n\,\delta^2)}{n}\right] \big(\langle \cos[(n-1)\,\xi] \rangle - \langle \cos[(n+1)\,\xi] \rangle\big), \tag{A8}$$

$$\langle Y^2 \rangle = 2\,(2\,k^2 - 1)\, \langle 1 \rangle - 2\, \langle \cos\xi \rangle, \tag{A9}$$

where $m > 1$, and use has been made of Eqs. (73)–(76).

We can write

$$C_0(k) = \begin{cases} K(k) & 0 \leq k \leq 1 \\ k^{-1}\, K(1/k) & k > 1, \end{cases} \tag{A10}$$

and[27,28]

$$C_n(k) = \begin{cases} \displaystyle\sum_{l=0,n} c_{n,l}\, k^{2(n-l)}\, S_{n-l}(k) & 0 \leq k \leq 1 \\ \displaystyle\sum_{l=0,n} c_{n,l}\, k^{-1}\, S_{n-l}(1/k) & k > 1, \end{cases} \tag{A11}$$

for $n > 0$. Here,

$$c_{n,l} = \frac{(-1)^l\, n\, (2\,n - l - 1)!\, 2^{2(n-l)}}{l!\, (2\,n - 2\,l)!}, \tag{A12}$$

and

$$S_n(k) = \int_0^{\pi/2} \frac{\sin^{2n}\theta}{\sqrt{1 - k^2\, \sin^2\theta}}\, d\theta. \tag{A13}$$

Finally,[29]

$$S_0(k) = K(k), \tag{A14}$$

$$S_1(k) = \frac{K(k) - E(k)}{k^2}, \tag{A15}$$

$$S_n(k) = \left(\frac{2n-2}{2n-1}\right)\left(\frac{1+k^2}{k^2}\right) S_{n-1}(k) - \left(\frac{2n-3}{2n-1}\right)\left(\frac{1}{k^2}\right) S_{n-2}(k), \tag{A16}$$

for $n \geq 2$, where

$$K(k) = \int_0^{\pi/2} (1 - k^2\, \sin^2\theta)^{-1/2}\, d\theta, \tag{A17}$$

$$E(k) = \int_0^{\pi/2} (1 - k^2 \sin^2\theta)^{1/2}\, d\theta, \tag{A18}$$

are complete elliptic integrals.[30] At small k, the $S_n(k)$ are more conveniently evaluated by means of the power series expansion[31]

$$S_n(k) = \frac{\pi}{2} \sum_{l=0,\infty} \frac{[(2\,(n+l)-1]!!\,(2\,l-1)!!}{[2\,(n+l)]!!\,(2\,l)!!}\, k^{2l}, \tag{A19}$$

for $n > 0$. At large k, the $C_n(k)$ are more conveniently evaluated by means of the power series expansion[32]

$$C_n(k) = \frac{\pi}{2} \sum_{l=n,\infty} \frac{(2\,l-1)!!\,(2\,l)!}{(2\,l)!!\,(l+n)!\,(l-n)!}\, \frac{1}{2^{2l}\,k^{2l+1}}, \tag{A20}$$

for $n > 0$.

Note, finally, that, in practice, the sums over the Fourier harmonics of ζ and ξ in Eqs. (107), (122), and Eqs. (A5)–(A8) cannot extend from $n = 0$ to ∞, but must, instead, be truncated at some maximum value of n, which is denoted N. It can be seen from Fig. 9 that truncation at $N = 15$ yields accurate results for island asymmetry factors less than about 0.8.

[1] J. A. Wesson, *Tokamaks*, 3rd ed. (Oxford University Press, 2004).
[2] A. H. Boozer, Rev. Mod. Phys. **76**, 1071 (2005).
[3] S. I. Braginskii, in *Reviews of Plasma Physics*, edited by M. A. Leontovich (Consultants Bureau, New York, NY, 1965), Vol. 1, p. 205.
[4] R. Fitzpatrick, Phys. Plasmas **2**, 825 (1995).
[5] J. P. Freidberg, *Ideal Magnetohydrodynamics* (Springer, 1987).
[6] H. P. Furth, J. Killeen, and M. N. Rosenbluth, Phys. Fluids **6**, 459 (1963).
[7] P. H. Rutherford, Phys. Fluids **16**, 1903 (1973).
[8] A. Thyagaraja, Phys. Fluids **24**, 1716 (1981).
[9] D. F. Escande and M. Ottaviani, Phys. Lett. A **323**, 278 (2004).
[10] R. J. Hastie, F. Militello, and F. Porcelli, Phys. Rev. Lett. **95**, 065001 (2005).
[11] Z. Chang and J. D. Callen, Nucl. Fusion **30**, 219 (1990).
[12] R. J. Bickerton, J. W. Connor, and J. B. Taylor, Nat. Phys. Sci. **229**, 110 (1971).
[13] R. Carrera, R. D. Hazeltine, and M. Kotschenreuther, Phys. Fluids **29**, 899 (1986).
[14] J. P. Meskat, H. Zohm, G. Gabentein, S. Günter, M. Maraschek, W. Suttrop, W. Yu, and ASDEX Upgrade Team, Plasma Phys. Controlled Nucl. Fusion **43**, 1325 (2001).
[15] E. Lazzaro and S. Nowak, Plasma Phys. Controlled Nucl. Fusion **51**, 035005 (2009).
[16] D. De Lazzari and E. Westerhof, Plasma Phys. Controlled Nucl. Fusion **53**, 035020 (2011).
[17] R. B. White, D. A. Gates, and D. P. Brennan, Phys. Plasmas **22**, 022514 (2015).
[18] D. A. Gates and L. Delgado-Aparicio, Phys. Rev. Lett. **108**, 165004 (2012).
[19] D. A. Gates, L. Delgado-Aparicio, and R. B. White, Nucl. Fusion **53**, 063008 (2013).
[20] D. A. Gates, D. P. Brennan, L. Delgado-Aparicio, and R. B. White, Phys. Plasmas **22**, 060701 (2015).
[21] D. A. Gates, D. P. Brennan, L. Delgado-Aparicio, Q. Teng, and R. B. White, Phys. Plasmas **23**, 056113 (2016).
[22] R. D. Hazeltine, M. Kotschenreuther, and P. J. Morrison, Phys. Fluids **28**, 2466 (1985).
[23] R. D. Hazeltine and J. D. Meiss, *Plasma Confinement* (Dover, 2003).
[24] M. N. Rosenbluth, R. D. Hazeltine, and F. L. Hinton, Phys. Fluids **15**, 116 (1972).
[25] D. Brouwer and G. M. Clemance, *Methods of Celestial Mechanics* (Academic Press, 1961), Chap. II.
[26] I. S. Gradshteyn and I. M. Ryzhik, *Table of Integrals, Series, and Products* (Academic Press, 1980). Sect. 3.719.
[27] E. W. Weisstein, see http://mathworld.wolfram.com/Multiple-AngleFormulas.html for Multiple-Angle Formulae. From MathWorld—A Wolfram Web Resource.
[28] E. W. Weisstein, see http://mathworld.wolfram.com/ChebyshevPolynomialoftheFirstKind.html for Chebyshev Polynomial of the First Kind. From MathWorld—A Wolfram Web Resource.
[29] I. S. Gradshteyn and I. M. Ryzhik, *Table of Integrals, Series, and Products* (Academic Press, 1980). Sect. 2.58.
[30] *Handbook of Mathematical Functions with Formulas, Graphs, and Mathematical Tables*, edited by M. Abramowitz and I. A. Stegun (Dover, 1965). Chap. 17.
[31] I. S. Gradshteyn and I. M. Ryzhik, *Table of Integrals, Series, and Products* (Academic Press, 1980). Sects. 1.11 and 3.62.
[32] I. S. Gradshteyn and I. M. Ryzhik, *Table of Integrals, Series, and Products* (Academic Press, 1980). Sects. 1.11 and 1.32.